We are IntechOpen, the world's leading publisher of Open Access books Built by scientists, for scientists

6,000
Open access books available

148,000
International authors and editors

185M
Downloads

Our authors are among the

154
Countries delivered to

TOP 1%
most cited scientists

12.2%
Contributors from top 500 universities

CLARIVATE ANALYTICS
BOOK CITATION INDEX
INDEXED

WEB OF SCIENCE™

Selection of our books indexed in the Book Citation Index
in Web of Science™ Core Collection (BKCI)

Interested in publishing with us?
Contact book.department@intechopen.com

Chapter

Development of Schizont Stages of *Toxoplasma gondii* in Primary Cell Culture of Feline Enterocytes

Renata M. de Muno, Marcos A. Moura, Letícia C. Medeiros, Pedro N. Caldas, Rafael M. Mariante and Helene S. Barbosa

Abstract

Intestinal epithelial cell cultures are a potentially applicable model for investigating enteropathogens such as the protozoan *Toxoplasma gondii*, the etiological agent of toxoplasmosis. Felids such as domestic cats are the only known definitive hosts where the parasite undergoes sexual reproduction, which occurs in the enterocytes. Primary feline intestinal epithelial cell (FIEC) cultures were obtained from the fetal small gut of felines, and the epithelial nature of these cells was confirmed by the revelation of cytokeratin and intestinal alkaline phosphatase content by fluorescence microscopy, besides alignment, microvilli, and adherent intercellular junctions by ultrastructural analysis. FIECs infected with *T. gondii* bradyzoite forms showed that the parasite:cell ratio was determinant for establishing the lytic cycle and cystogenesis and the induction of schizont-like forms. Type C and D schizonts were identified by light and electron microscopies, which showed morphological characteristics like those previously described based on the analysis of cat intestines experimentally infected with *T. gondii*. These data indicate that FIECs simulate the microenvironment of the felid intestine, allowing the development of schizogony and classic endopolygeny. This cellular framework opens new perspectives for the *in vitro* investigation of biological and molecular aspects involved in the *T. gondii* enteric cycle.

Keywords: *Toxoplasma gondii*, enteric cycle, primary cell culture, feline enterocytes, schizont stages

1. Introduction

Intestinal cells act as barriers to prevent access to potentially harmful substances and the migration of the underlying cells in the lamina propria [1]. Several investigators have established culture methods for intestinal cells from different animal species that mimic normal intestinal development [2]. Culture techniques have been developed for cells from different sources, including adult [3, 4] and embryonic cells [5–8]. The introduction of growth factors or interaction of these systems with the extracellular matrix during recent decades has allowed the development of experimental approaches to study *in vitro* differentiation [9, 10]. These advances have afforded the

possible application of enterocyte cultures for *in vitro* studies (e.g., the interaction of these cells with enteroparasites [11] such as *Toxoplasma gondii* [8]).

T. gondii, the etiological agent of toxoplasmosis, is an obligatory intracellular parasite that causes one of the most common zoonoses in the world. Its transmission occurs by (i) oral infection via the ingestion of cysts, present in raw or poorly cooked meat; (ii) ingestion of oocysts, present in the feces of Felidae contaminating food, water, and soil [12, 13]; or (iii) vertical transmission via the transplacental route [14, 15]. Cats and other felines are the only definitive hosts capable of directly spreading *T. gondii* in the environment, since the enteroepithelial cycle, including the sexual stage of the parasite, occurs exclusively in those species [16]. The infection in felids is established after ingestion of cysts or oocysts in tissues whose walls are destroyed by proteolytic enzymes in the stomach and intestine, resulting in the release of bradyzoites or sporozoites that invade intestinal cells and initiate the enteroepithelial cycle of the parasite [17].

Five distinct enteroepithelial morphological stages or schizonts of *T. gondii* (Types: A, B, C, D, and E) are described in the felid gut, involving the processes of schizogony, gametogony, and sporogony, which result in the formation of immature oocysts [16–19]. Specific knowledge about the enteric cycle of *T. gondii* in Felidae is limited to morphological characterization *in vivo* [17, 20–25], which makes it difficult to monitor the kinetics of infection. Thus, the analysis of the temporal events established during this *in vivo* cycle is subjective since histological studies of the gut do not allow monitoring the actual sequence of differentiation events of the parasite's infectious stages. However, the practice of euthanasia of cats for scientific studies is restricted [26], which corroborates the need to introduce alternative research models to explore the enteroepithelial cycle of *T. gondii* in felids.

No cell models of the feline intestinal epithelium are commercially available to allow the study of the *T. gondii* enteroepithelial cycle *in vitro*. Several attempts to culture intestinal epithelial cells from adult animals or establish normal cell lines derived from normal enterocytes have not been very successful [27]. The lack of cellular models that allow the reproduction of the enteric cycle of *T. gondii* in felids motivated us to introduce primary cultures of cat enterocytes as an alternative for this study. Preliminary data from this interaction have been published by our group [8]. We now deepen this study by revealing the *T. gondii* development *in vitro* in feline enterocytes.

2. Experimental design

2.1 Feline enterocyte primary cell culture

Feline enterocyte primary cell cultures (FIEC) were obtained from fetuses of a clinically healthy pregnant domestic cat (no gastrointestinal disease and serologically negative for *T. gondii*, feline immunodeficiency virus, and feline leukemia virus). All procedures were performed in accordance with the guidelines stipulated by the Brazilian College of Animal Experimentation (COBEA). This study was approved by the Fundação Oswaldo Cruz Committee of Ethics for the Use of Animals (license L042/2018 A1).

Small intestine samples corresponding to the jejunum-ileum region (~5 cm) were collected aseptically. The samples were dissected, and the fragments were gathered in ice-cold sterile phosphate-buffered saline (PBS) with a 10% antibiotic solution (Sigma-Aldrich-St. Louis, MO, United States). This tissue was opened longitudinally,

washed three times with PBS, and maintained in this solution with 10% antibiotics for 20 min at room temperature. Fragments were divided into small pieces (1 cm^3) and washed into PBS. The fragments were placed in nonenzymatic dissociation buffer (pH 7.2) containing 1 mM EDTA (Sigma-Aldrich-St. Louis, MO, United States), 1 mM EGTA (Sigma-Aldrich-St. Louis, MO, United States), 0.5 mM dithiothreitol (Sigma-Aldrich-St. Louis, MO, United States), and 10% antibiotic solution for 20 min under stirring at room temperature [2–6]. The cell aggregates were plated in DMEM/Hams medium Dulbecco's Modified Eagle's Medium/Ham's Nutrient F12 (1:1) containing 1% antibiotic solution, 1 mM glutamine, 5% fetal bovine serum (Life Technologies, São Paulo, SP, Brazil), 20 ng/ml epidermal growth factor (Sigma-Aldrich-St. Louis, MO, United States) [4, 7], 0.1% human insulin (Humulin N - Lilly, Indianapolis, IN, United States), 100 nM hydrocortisone (Sigma-Aldrich-St. Louis, MO, United States), 1% nonessential amino acids 100x (Life Technologies, São Paulo, SP, Brazil), and 1 μg/ml 3,3′, 5-triiodo-L-thyronine sodium salt (Sigma-Aldrich-St. Louis, MO, United States) [10]. The cultures were maintained at 37°C in a 5% CO_2 atmosphere, and the medium was renewed every two days.

Confluent FIECs were treated for 10 min at 37°C with dissociation solution (PBS with 0.01% EDTA and 0.25% trypsin). After dissociation, the cells were placed in culture medium at 4°C with 10% fetal bovine serum to inhibit the action of trypsin, centrifuged for 7 min at 650 × *g* at 4°C, and grown in 24-well plates on coverslips (10^5 cells/well) or on 35 mm^3 plastic disks (5.0 x 10^5 cells/disk). Cell cultures were daily analyzed by light microscopy (Zeiss Imager A2 microscope) after fixation in Bouin's solution and Giemsa staining to assess morphology and proliferation. Images were captured with Soft Axion Vision 40 v.4.8.2.0 and an Axion cam MRc color camera.

2.2 Characterization of FIEC by immunolabeling

Several monoclonal antibodies were applied to characterize the FIECs: anti-pan-cytokeratin clone PCK-26 (Sigma-Aldrich-St. Louis, MO, United States); anti-vimentin clone VIM-13.2 (Sigma-Aldrich-St. Louis, MO, United States); anti-intestinal alkaline phosphatase clone AP-59 (Sigma-Aldrich-St. Louis, MO, United States); and anti-desmin clone DE-U-10 (Sigma-Aldrich-St. Louis, MO, United States). The cells were fixed for 10 min at 4°C with 4% paraformaldehyde in PBS, washed three times for 10 min in PBS, and then incubated for 30 min in 50 mM ammonium chloride to block free aldehyde radicals. Afterward, the cells were permeabilized for 20 min in a PBS solution containing 0.05% Triton X-100 (Roche, Rio de Janeiro, RJ, Brazil) and 4% BSA (Sigma-Aldrich-St. Louis, MO, United States) to block nonspecific binding. For the indirect immunofluorescence assays, the cells were incubated for 2 h at 37°C with the following primary antibodies: anti-vimentin (1:200); anti-cytokeratin (1:100); anti-intestinal alkaline phosphatase; and anti-desmin (1:100). After this incubation, the cells were washed 3 times for 10 min in PBS containing 4% BSA and incubated for 1 h at 37°C with the secondary antibody at a dilution of 1:1000 (mouse anti-IgG conjugated with FITC or TRITC) (Sigma-Aldrich-St. Louis, MO, United States). To reveal actin filaments, the cells were incubated for 1 h at 37°C with 4 μg/mL phalloidin-FITC in PBS (Sigma-Aldrich-St. Louis, MO, United States). Next, the cultures were washed 3 times for 10 min in PBS and incubated for 5 min with 0.1 μg/mL 4′,6-diamidino-2-phenylindole (DAPI, Sigma-Aldrich-St. Louis, MO, United States) diluted in PBS. After wash, the coverslips were mounted on slides with a solution of 2.5% DABCO (1,4-diazabicyclo-[2,2,2]-octane-triethylenediamine)

(Sigma-Aldrich-St. Louis, MO, United States) in PBS containing 50% glycerol, pH 7.2. Controls were performed by omission of the primary antibody. The samples were examined with a confocal laser-scanning microscope (CLSM Axiovert 510, META, Zeiss) with a 543 helium laser (LP560 filter), 488 argon/krypton laser (Ar/Kr) (filter LP515), and a 405 Diode laser (LP 420 filter).

2.3 Isolation of *T. gondii* bradyzoites and interaction with FIEC

T. gondii cysts from the ME-49 strain (Type II) previously isolated from infected mice were inoculated intraperitoneally into female C57BL/6 mice (15–18 g) with 50 cysts/animal. Four and 12 weeks after infection, the mice were sacrificed and the brain cysts isolated, as described by Freyre [28] and modified by Guimarães et al. [29]. In addition, bradyzoites were obtained from isolated tissue cysts according to Popiel et al. [30].

Confluent FIEC cultures were infected with *T. gondii* bradyzoites. The assays were performed at 1:5, 1:10, and 1:20 (parasite: host cell) ratios for periods ranging from 1 to 9 days postinfection to analyze the infection course and to evaluate the parasite's intracellular fate. After different periods of interaction, the cells were washed in PBS and processed according to the experiments to be performed.

The ability of the *T. gondii* bradyzoites to infect FIECs *in vitro* was examined by fixation of the cells in Bouin's solution and Giemsa staining. The infection analysis was carried out with 200 cells per coverslip in three independent experiments at interaction times of 24, 48, 72, and 96 hours, in duplicate. Data were analyzed in GraphPad Prism 7.0 using Two-Way ANOVA with Tukey's multiple comparisons test, and results were expressed as mean with SEM (graph) or SD (table). Differences were considered statistically significant when the p-value was <0.05.

2.4 Characterization of *T. gondii* stages by immunolabeling

The differentiation of parasites in culture cells infected with bradyzoite forms of *T. gondii* was monitored using tachyzoite stage-specific anti-SAG-1 antibodies (kindly provided by Dr. José Roberto Mineo - Immunoparasitology Laboratory, Federal University of Uberlândia, Minas Gerais, Brazil). Bradyzoites of *T. gondii* were identified with stage-specific anti-BAG-1 antibodies (anti-BAG1-7E5; kindly supplied by Dr. Wolfgang Bohne - Institut für Medizinische Mikrobiologie, Universität Göttingen, Germany) as previously described [31]. Initially, the cultures were fixed for 20 min at 4°C on days 1 to 4 with 4% PFA in PBS, washed three times for 10 min in PBS, and then incubated for 30 min in 50 mM ammonium chloride to block free aldehyde radicals. Next, the cells were permeabilized for 20 min in a PBS solution containing 0.05% Triton X-100 (Roche, Rio de Janeiro, RJ, Brazil) and 4% BSA (Sigma-Aldrich-St. Louis, MO, United States) to block nonspecific binding. For the indirect immunofluorescence assay, the host cells were incubated for 2 h at 37°C with the primary antibodies anti-SAG-1 (1:200) and anti-BAG (1:500) diluted in PBS/BSA. After incubation, the cells were washed with PBS containing 4% BSA and incubated for 1 h at 37°C with the secondary antibody at a 1:1000 dilution (anti-mouse IgG conjugated with FITC). Controls were performed by omission of the primary antibodies. Afterward, the cultures were washed 3 times for 10 min in PBS and processed for fluorescence microscopy as described above.

2.5 Ultrastructural analysis

FIECs infected or not with bradyzoite forms of *T. gondii* were washed 3 times for 10 min with PBS and fixed for 1 h at 4°C in 2.5% glutaraldehyde diluted in a 0.1 M sodium cacodylate buffer containing 3.5% sucrose and 2.5 mM $CaCl_2$ (pH 7.2). After fixation, the cells were washed in the same buffer and then post-fixed for 30 min at room temperature in 1% osmium tetroxide diluted in a 0.1 M Na-cacodylate buffer. For transmission electron microscopy analysis, the cells were washed in the same buffer, scraped from the plastic dish at 4°C, and centrifuged. Then, the cells were dehydrated in a graded acetone series and embedded in an epoxy resin (PolyBed 812). Thin sections were stained with uranyl acetate and lead citrate and then examined under a transmission electron microscope (Jeol JEM1011). For scanning electron microscopy, the FIECs were fixed for 30 min at room temperature with 2.5% glutar-aldehyde in 0.1 M Na-cacodylate buffer (pH 7.2) and post-fixed for 30 min at room temperature with a solution of 1% OsO4 containing 2.5 mM $CaCl_2$ in the same buffer. The cells were dehydrated in an ascending acetone series and dried by the critical point method with CO_2 (CPD 030, Balzers, Switzerland). The samples were mounted on aluminum stubs, coated with a 20 nm layer of gold (Cressington Sputter Coater 108), and examined under a scanning electron microscope (Jeol JSM 6390LV) at the Rudolf Barth Electron Microscopy Platform at Oswaldo Cruz Institute.

3. Results

3.1 Morphological characteristics of feline intestinal cells *in vitro*

The attachment of FIECs to the substrate was observed by phase-contrast micros-copy, in situ. In 5 days, the cells aligned and polarized, with the nuclei located in the same plane as the organization of the columnar epithelium (**Figure 1A**). Ultrastructural analysis by scanning electron microscopy showed the absorptive characteristics of these cells, including the identification of plasma membrane projections that established focal adhesion points (**Figure 1B**). Long and thin finger-like projections were visible and often established cell-cell contacts and extensive cytoplasmic contacts, indicating the forma-tion of specialized membrane areas, such as cellular junctions (**Figure 1B**). Transmission electron microscopy demonstrated that epithelial cells in culture retained a great number of cytological features typical of intestinal epithelial cells, such as large numbers of microvilli (i.e., a brush border at the apical pole) (**Figure 1C–D**). Lateral interdigita-tions are observed below the junctional complex between two adjacent epithelial cells (**Figure 1C**). The junctional areas presented tight junctions (zonula occludens) in which the outer leaflets of the plasma membranes were fused, intermediate junctions (zonula adherens), characterized by plasma membranes separated by a space, and desmosomes (macula adherens) (**Figure 1D**). All these characteristics confirmed the intestinal epithelial nature of FIECs as enterocytes that were maintained for up to six passages.

3.2 Expression of intestinal markers in FIEC

To confirm the epithelial nature of FIEC, we investigated the intermediate filaments by employing an anti-pan-cytokeratin antibody that recognizes a range of cytokeratins (1, 5, 6, 8, and 10). Confocal laser scanning microscopy showed that secondary cultures
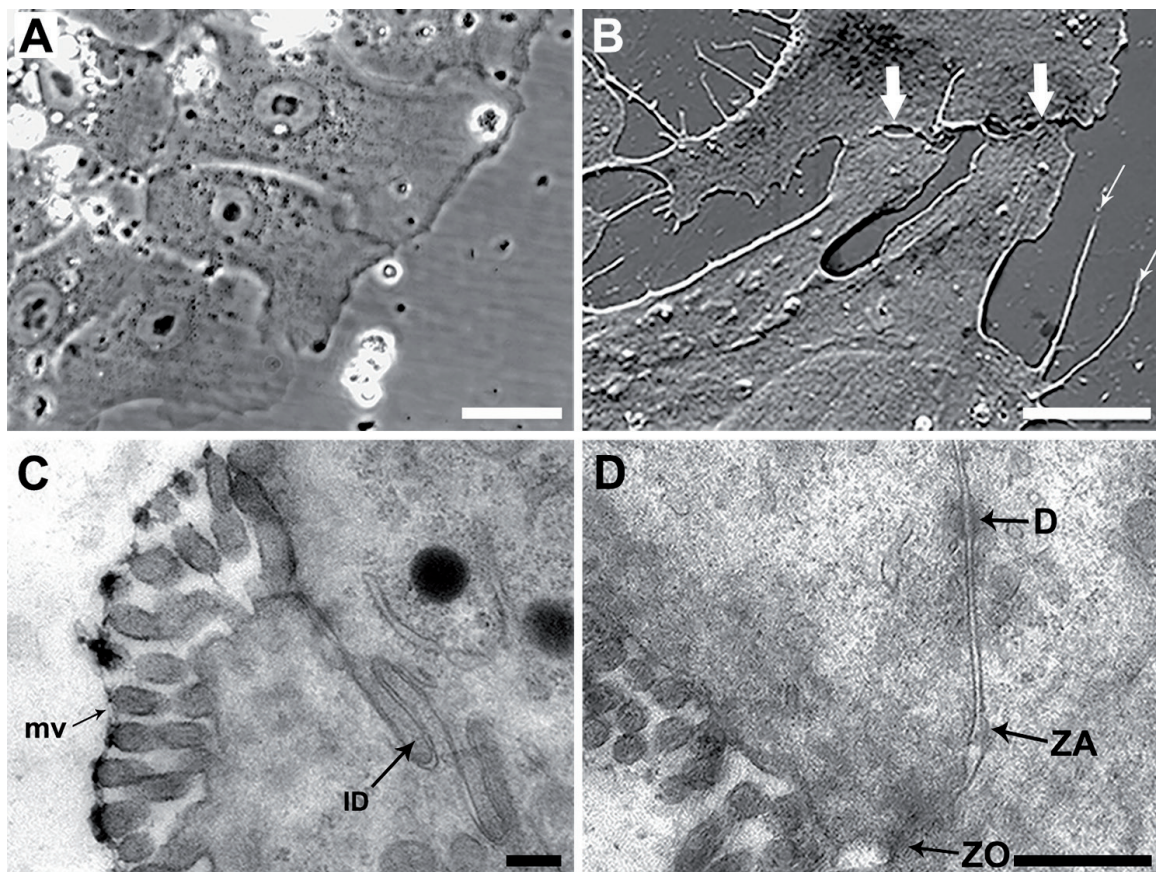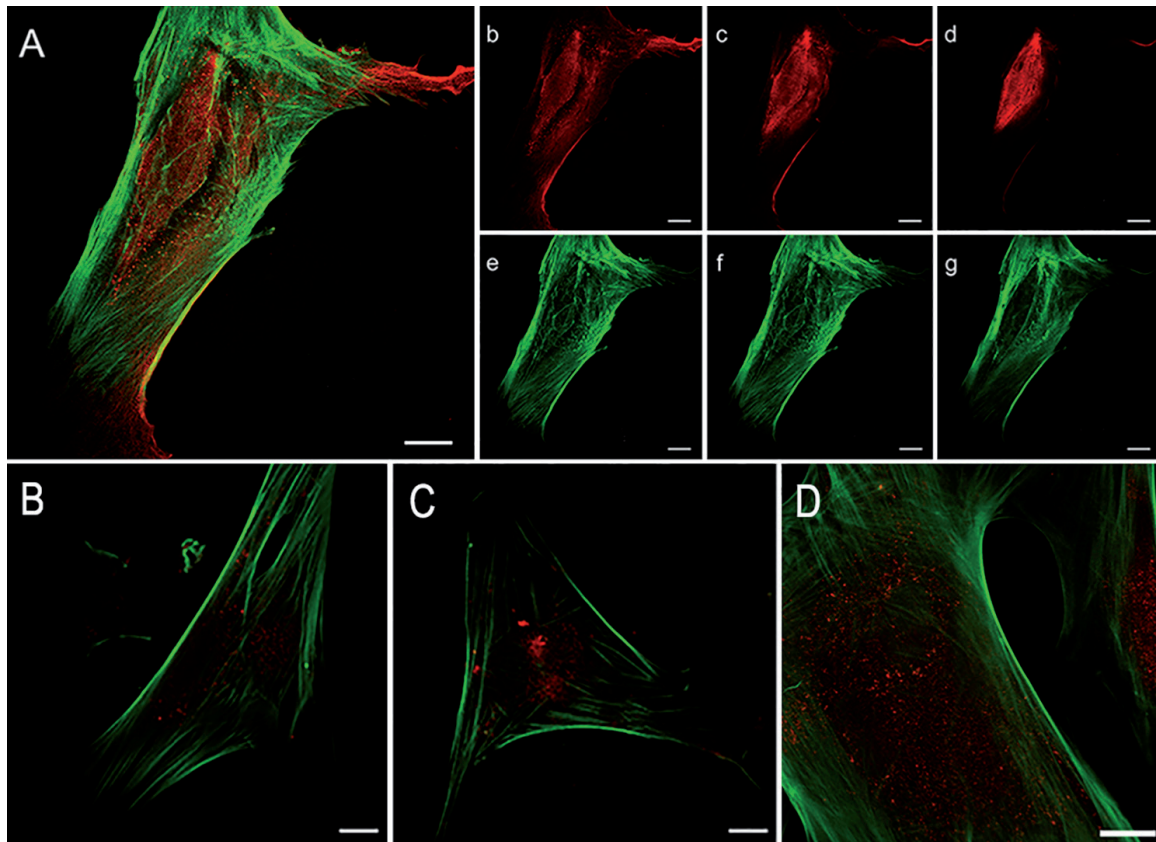
Figure 1.
Morphological characterization of cells isolated from felid small intestines. (A) Cells with 24 h of cultivation showed epithelial characteristics, such as alignment and polarization. The nuclei of the cells are located in the same plane, similar to the organization of the intestinal epithelium. (B) Scanning electron microscopy revealed thin and long cytoplasmic projections and focal points of adhesion to the substrate (thin arrows). Cell-cell contact areas form specialized contact points, such as intercellular junctions (thick arrows). (C-D) By transmission electron microscopy, many microvilli (mv) are observed at the apical pole. Junctional complex areas (ZO = zonula occludens; ZA = zonula adherens; D = desmosomes) are located at interdigitations. Bars: (A) 20 µm; (B) 5 µm; (C) 0.5 µm; (D) 0.2 µm.

of FIECs preserved the morphological and functional characteristics of immature enterocytes. These cells sustained strong expression of cytokeratin concentrated around the nuclei after two weeks, indicating they were truly epithelial (**Figure 2A–D**). Double staining by phalloidin-FITC to identify actin filaments and the anti-cytokeratin antibody revealed little to no co-localization between these proteins (**Figure 2A**). The localization of actin filaments was mostly observed at focal adhesion points for the substrate at the cellular membrane (**Figure 2A–G**). The functional properties of FIECs were evaluated based on the expression of intestinal alkaline phosphatase, which is an enzyme secreted by the intestinal epithelium (**Figure 2B–D**). Intestinal alkaline phosphatase expression was initially detected after 5 days of culture (**Figure 2B**). The labeling showed a progressive increase in the enzyme concentration inside the cells, which occurred between 7 and 9 days post-cultivation (**Figure 2C–D**). The immunocytochemistry assays targeting vimentin and desmin failed in the FIECs until up to 15 days in secondary culture (data not shown), as expected for healthy intestinal cells.

3.3 *T. Gondii* bradyzoite-FIEC interaction *in vitro*

Previously, we described the behavior of bradyzoites during their interaction with FIECs [8]. Here, quantitative and qualitative analyses were performed with ratios
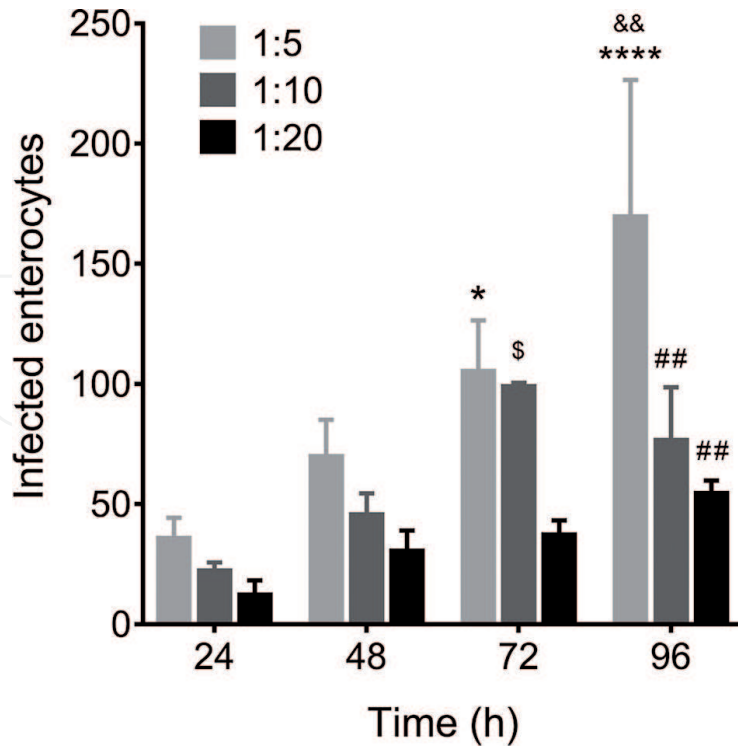
Figure 2.
Characterization of FIEC by fluorescence microscopy. (A) Culture of FIECs presenting epithelial morphology, revealed by double labeling: Actin filaments in green and cytokeratin in red. (b–d) Cytokeratin expression is located around the nucleus. (e–g) Actin filament organization revealed by phalloidin in FIECs shows the cell morphology and the major concentration at the focal adhesion points. (B–D) Intestinal alkaline phosphatase immunoreactivity in FIECs (red), shows activity that progressively increased in the cells as a function of the culture time. (B) 5 days, (C) 7 days, and (D) 9 days post-seeding. Actin filaments are shown in green. Bars: 20 μm.

of 1:5, 1:10, and 1:20 (parasite: host cell). The number of infected cells was analyzed after 24 to 96 h of parasite and host cell interaction (**Figure 3**). The data indicated the influence of the parasite load on the number of infected enterocytes during the study period: 9% after 24 hours of interaction and 42.4% after 96 hours when the 1:5 ratio was used (**Table 1**). Ratios of 1:10 and 1:20 (parasite: host cell) resulted in a lower number of infected enterocytes when compared to the 1:5 ratio. The main difference between the 1:10 and 1:20 ratios was the occurrence of structures similar to cysts (cyst-like) or schizonts (schizont-like), as previously observed by our group [8]. Cyst-like structures were more common when the ratio of 1:10 was employed, while the ratio of 1:20 resulted in more schizonts-like structures (**Table 1**).

The analysis of the parasite-host cell interaction with the 1:5 ratio revealed that the parasites doubled during the first 24 h of infection, with rosette form indicating the occurrence of endodyogeny, as seen by Giemsa (**Figure 4A**) and immunofluorescence, revealing tachyzoites with anti-SAG antibodies (**Figure 4B**). The bradyzoite-tachyzoite conversion occurred as shown by staining with the anti-SAG1-TRITC antibody (**Figure 4B**). After 96 hours of interaction, parasites were found in the extracellular environment, characterizing the lytic cycle of *T. gondii*, as seen by Giemsa (**Figure 4C**) and immunofluorescence (**Figure 4D**).

The establishment of *T. gondii* cystogenesis with the ratio of 1:10 was confirmed (**Figure 5**). Cyst-like intracellular structures in enterocytes were visible after 48 h
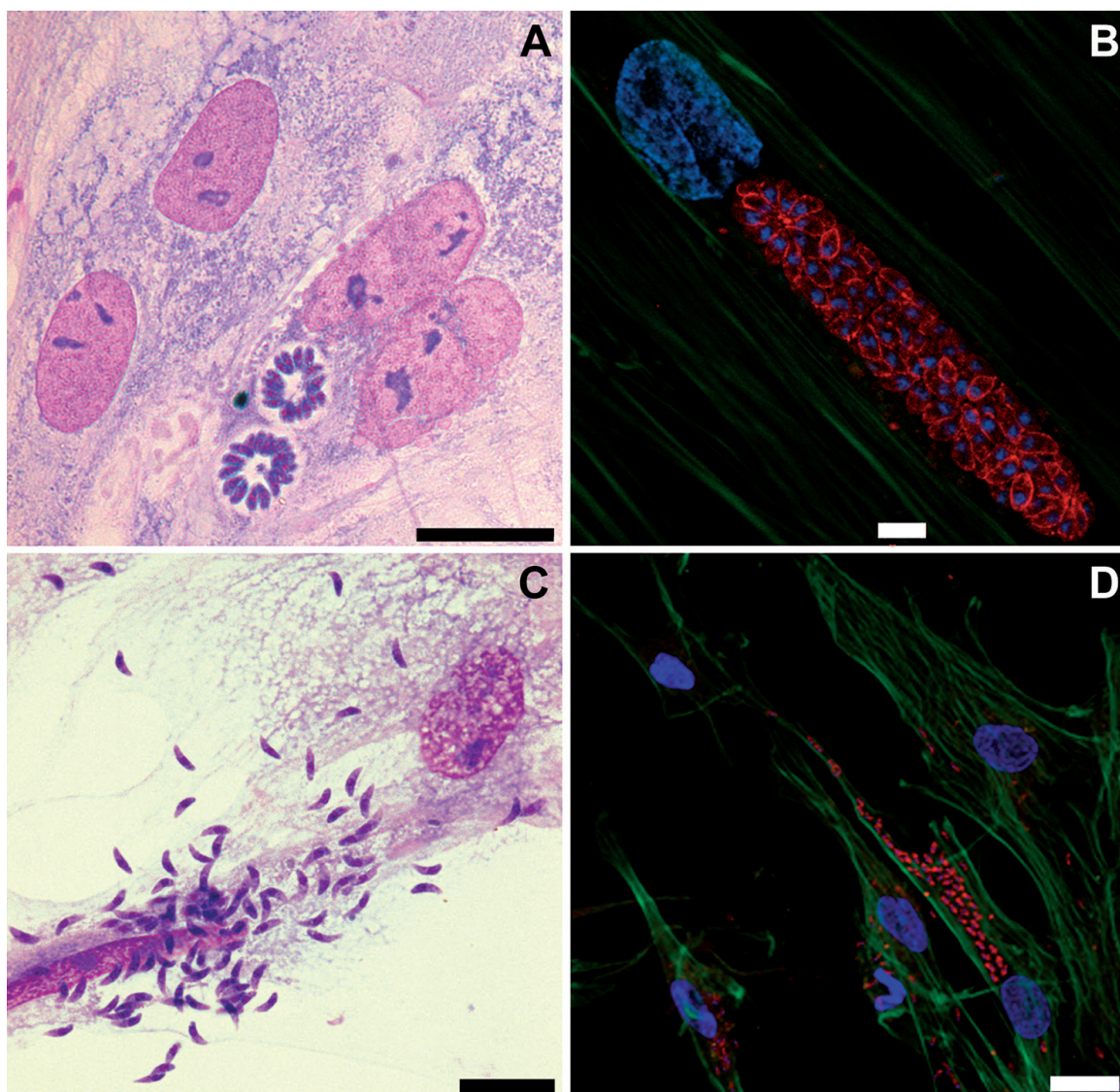
Figure 3.
*Absolute number of FIECs infected with T. gondii ME-49 strain bradyzoites. A total number of 400 cells were counted for each coverslip. The parasite-host cell ratios (MOI) were 1:5, 1:10 and 1:20. **** p < 0.0001 and * p < 0.05 compared to 24 h at MOI 1:5. && p < 0.01 compared to 48 h at MOI 1:5. $ p < 0.05 compared to 24 h at MOI 1:10. ## p < 0.01 compared to MOI 1:5 at 96 h.*

| Hours of interaction	Parasite:host cell ratio (MOI)	% Infected cells (IC)		% Cyst-like (CL)		% Schizont-like (SL)	
		Mean	SD	Mean	SD	Mean	SD
24	1:5	9.0	3.6	0	0	0	0
	1:10	5.6	1.5	0	0	0	0
	1:20	3.1	2.6	0	0	0	0
48	1:5	17.5	6.6	1.4	2.4	0	0
	1:10	11.4	3.8	11.7	10.2	0.8	1.4
	1:20	7.7	3.6	11.2	15.6	5.4	1.9
72	1:5	26.3	9.2	2.6	1.1	0	0
	1:10	24.8	0.7	32.1	16.0	0.7	1.2
	1:20	9.3	2.6	24.4	21.0	12.9	6.1
96	1:5	42.4	24.6	1.9	1.0	0	0
	1:10	19.2	9.5	75.3	76.2	0	0
	1:20	13.7	2.2	17.0	26.9	7.6	3.4

Table 1.
*Quantitative analyses of cyst-like and schizont-like forms during FIEC infection with ME49 T. gondii bradyzoites. Time comparison of IC for MOI 1:5: 96 h x 24 h ****, 96 h x 48 h **, 72 h x 24 h *. Time comparison of IC for MOI 1:10: 72 h x 24 h *. MOI comparison of IC for 96 h: 1:20 x 1:5 and 1:10 x 1:5 **. Time comparison of SL for MOI 1:20: 72 h x 24 h ****; 96 h x 24 h and 72 h x 48 h ***; 96 h x 72 h and 48 h x 24 h **. Time comparison of CL for MOI 1:10: 96 h x 24 h **; 96 h x 48 h *. MOI comparison of SL for 48 h: 1:20 x 1:10 and 1:20 x 1:5 *. MOI comparison of SL for 72 h: 1:20 x 1:10 and 1:20 x 1:5 ****. MOI comparison of SL for 96 h: 1:20 x 1:10 and 1:20 x 1:5 ***. MOI comparison of CL for 96 h: 1:20 x 1:10 *; 1:10 x 1:5 **. * p < 0.05, ** p < 0.01, *** p < 0.001, **** p < 0.0001.*

Figure 4.
Light microscopy of feline enterocytes infected with bradyzoites of T. gondii (1:5 parasite:host cell ratio). (A) Parasitophorous vacuoles show parasites in classic rosettes, indicating the interconversion from bradyzoites to tachyzoites. (B) Immunostaining for SAG1 (in red) reveals tachyzoites in FIECs and actin filaments (in green) with phalloidin. (D, E) The establishment of the lytic cycle was observed at 96 h provoked by tachyzoite proliferation based on Giemsa staining and immunolabeling with anti-SAG1 antibody. Bars: 20 μm.

(**Table 1**) by differential interference contrast microscopy (**Figure 5A**), staining with Giemsa (**Figure 5B**), and confirmed by ultrastructural analysis showing cyst wall, bradyzoites containing various granules of amylopectin and electron-dense rhoptries (**Figure 5C**).

As described during the quantitative analyses, schizont-like forms of *T. gondii* were observed in FIECs with the 1:20 ratio (**Table 1**). Starting at 48 h, cultures stained with Giemsa presented large parasitophorous vacuoles containing multinucleated masses (**Figure 6**). These structures had wide variability of shape and size, resembling the schizonts found in the gut of felines during the process of schizogony. It was common to observe more than one of these multinucleated masses (**Figure 6A, E**) and cell division processes by endodyogeny and schizogony in the same cell (**Figure 6D, E**). These structures are characterized as C-type schizonts, as advocated by Speer & Dubey [25], in a process of multiple nuclear division, with migration from the nuclei to the periphery, as can be seen in **Figure 6A–D**. This process of schizogony gives rise to merozoites,
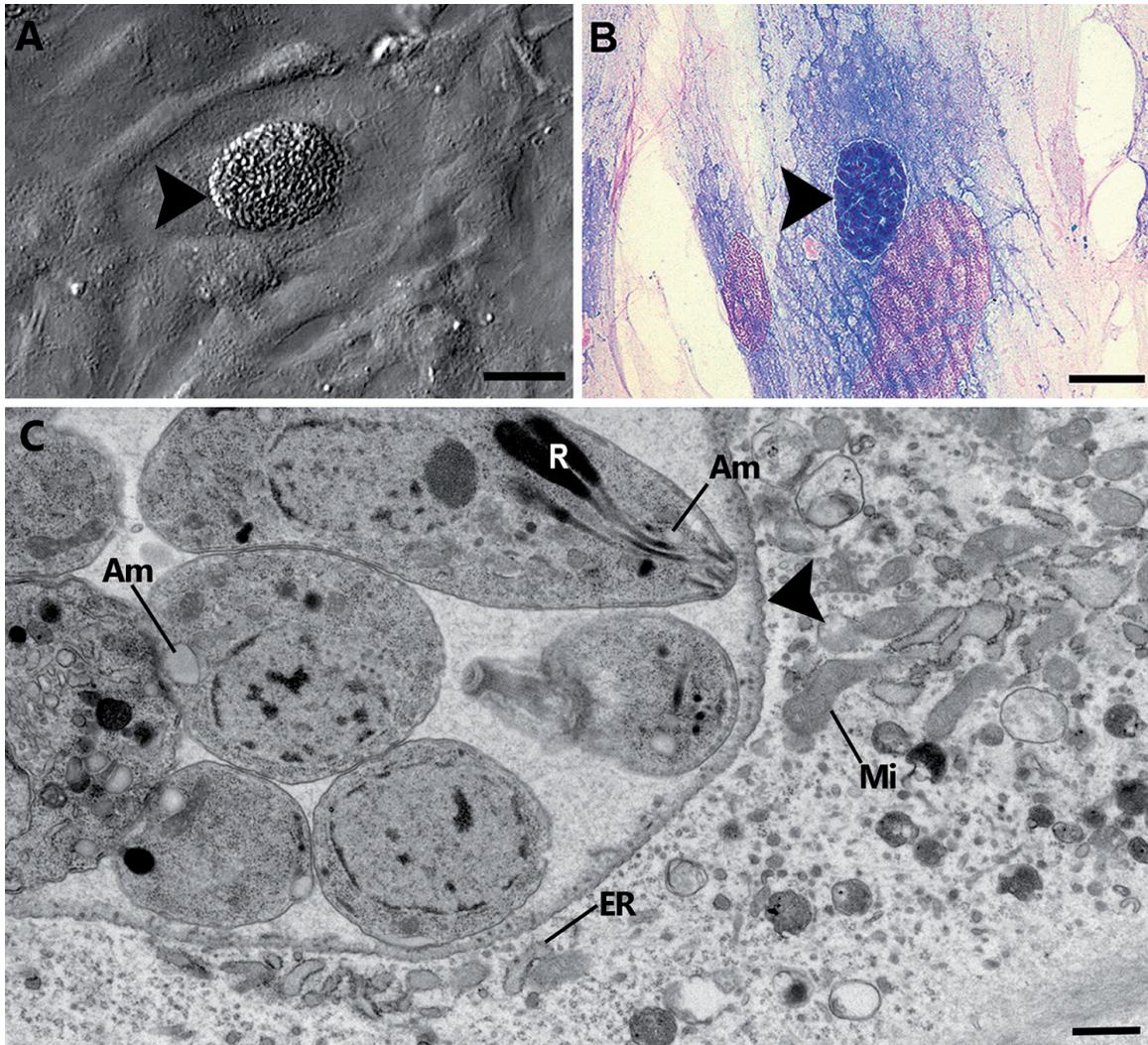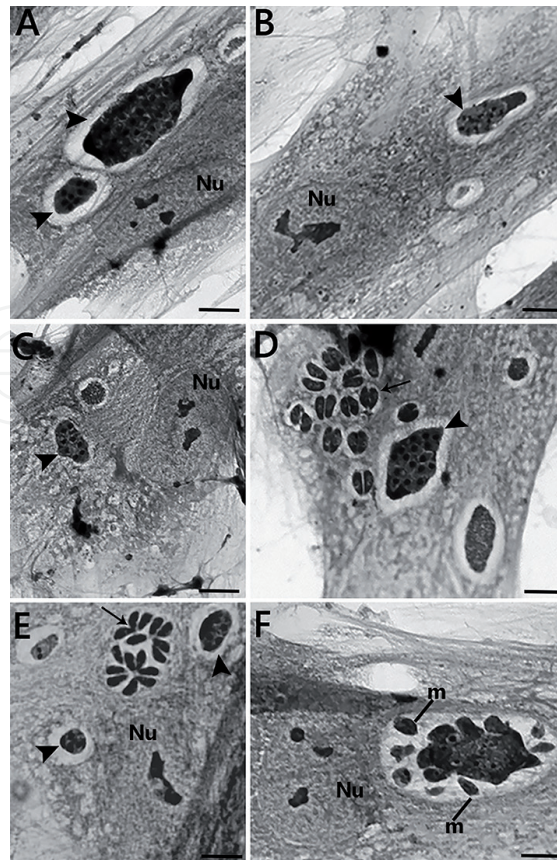
Figure 5.
Cysts of T. gondii in FIECs infected with the 1:10 bradyzoites:host cell ratio. (A-B) Differential interference contrast (DIC) microscopy (A) and Giemsa staining (B) show cyst-like structures (arrowheads) after 72 hpi (C) Cyst of T. gondii revealed by TEM with the cyst wall (arrowhead), parasites containing amylopectin granules (Am), and electron-dense rhoptries (R). ER = endoplasmic reticulum; Mi = mitochondria. Bar: (a, B) 20 µm; (C) 0.5 µm.

which are organized immediately below the schizont's membrane, as in a "budding," as suggested by **Figure 6F**. These will be better presented during the ultrastructural analyses. With the advancement of schizogony, the merozoites acquired a peripheral arrangement (**Figure 7A–D**) with the presence (**Figure 7B–D**) or not of a residual body (**Figure 7A**). The occurrence of different pathways of intracellular fate of the parasite was observed in a single cell: lytic cycle with formation of rosettes (**Figure 7B, D**) simultaneously to vacuoles containing C-type schizonts (**Figure 7A–D**).

Another type of schizont detected in enterocytes *in vitro,* according to the description of *in vivo* models, was a group of three or four parasites in a parallel arrangement, with or without residual body, identified as D-type schizonts. These structures were seen in PV isolated in the cytoplasm of cells, along with other PV-containing C-type schizonts of *T. gondii* (**Figure 8**).

Ultrastructural analysis of these infected cultures for periods ranging from 48 h to 9 days showed PV containing parasites with morphological characteristics similar to those of *T. gondii* enteroepithelial stages. Evidence of schizonts containing merozoites supports the suggestion that partial reproduction of the enteric cycle of *T. gondii* was

Figure 6.
Enterocytes infected with T. gondii bradyzoites of the ME-49 strain for 48 h. It is possible to observe several multinucleated masses of varied shapes and sizes in large vacuoles, corresponding to type C schizonts (arrowheads). (D, E) The same cell presents parasites in pairs (arrow in D) or rosettes (arrow in E) in process of cell division, corresponding to the lytic cycle, and vacuoles containing multinucleated masses (arrowheads). (F) Type C schizont showing merozoites (m) emerging from the multinucleated mass. Nu = enterocyte nucleus. Bars: 10 μm.
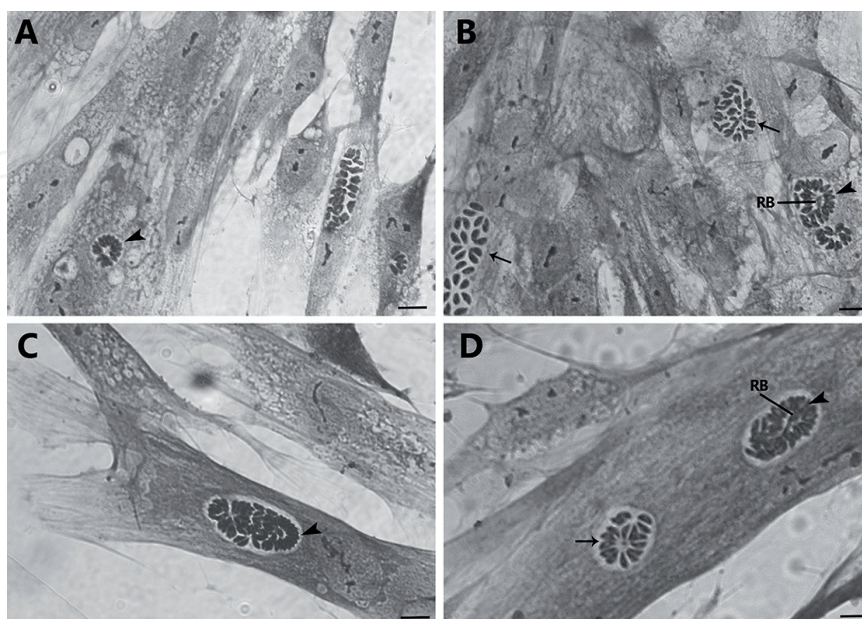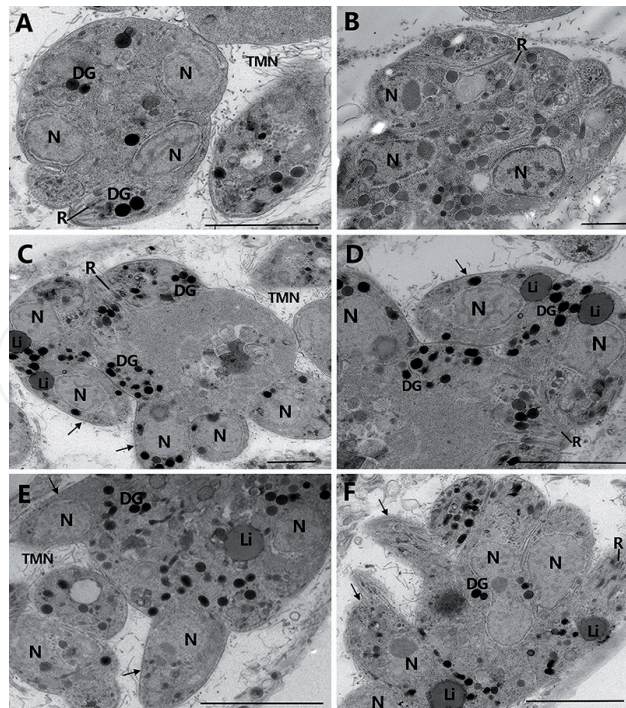

Figure 7.
Enterocytes infected with T. gondii bradyzoites of the strain ME-49 for 72 h. Note the presence of parasitophorous vacuoles that are morphologically smaller, along with peripherally arranged parasites inside the vacuoles with or without a large residual body (RB), as described for type C schizonts (arrowhead). Other vacuoles containing parasites in different stages of development can be seen in neighboring cells or in the same cell (arrows). Bars: 10 μm.
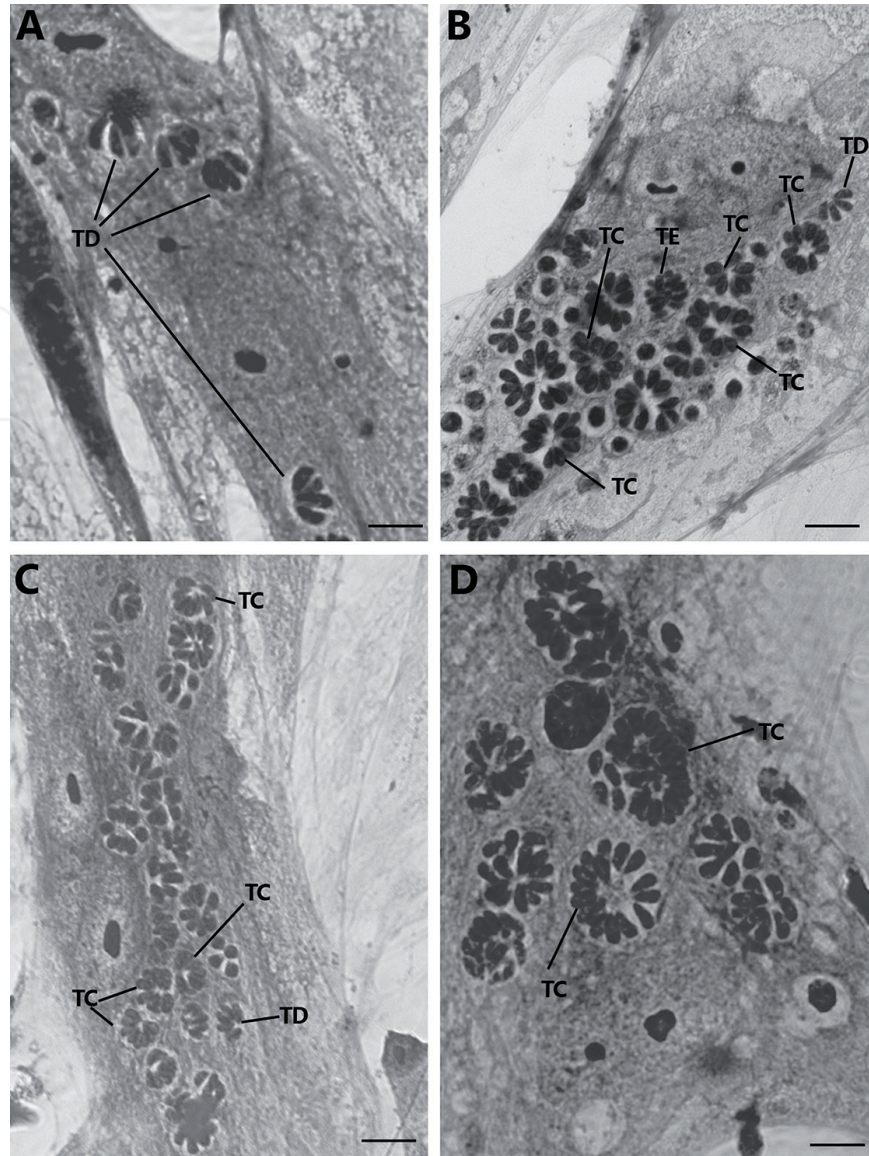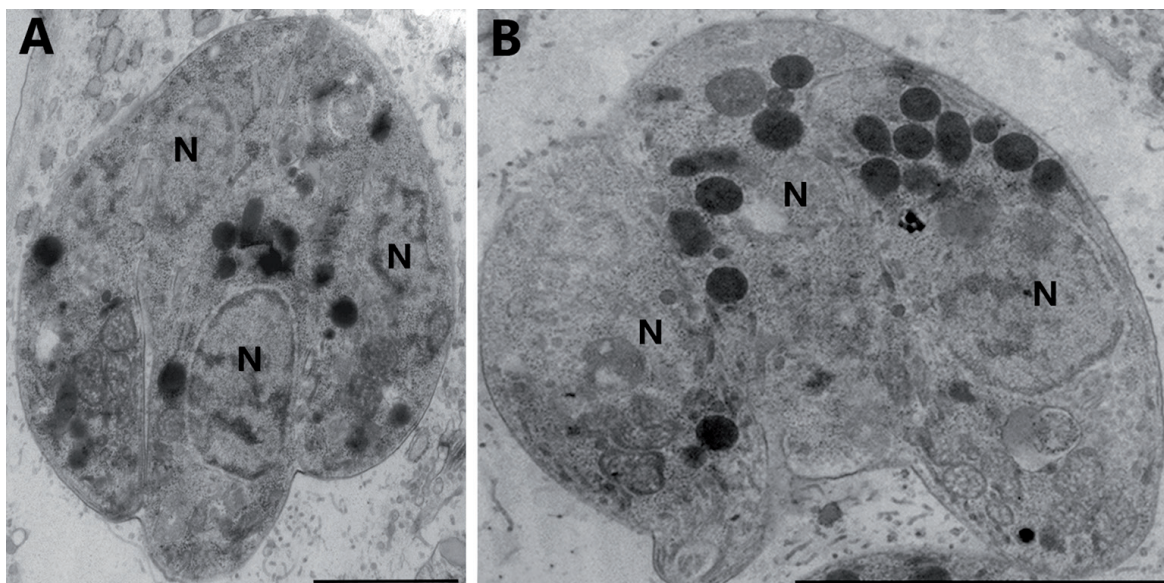
Figure 8.
Enterocytes infected with T. gondii bradyzoites of the strain ME-49 for 96 h. (A–C) Images suggestive of type D schizonts (TD) in groups of 3–4 parasites with or without residual bodies. (B–D) Several vacuoles containing parasites in different stages of cell division and development. Type C schizonts (TC) show parasites arranged peripherally inside the parasitophorous vacuoles. Bars: 10 μm.

obtained *in vitro*, as will be detailed below. Electron micrographs showed enterocytes with multinucleated structures that correspond to the C-type schizont forms (**Figure 9**), similar to those detected here by light microscopy stained with Giemsa (**Figure 6**).

The ultrastructural morphological characteristics of these multinucleated masses showed a varying number of nuclei in each of these structures, with diverse sizes and shapes, higher incidence of rounded shapes, presence of voluminous dense granules, and lipid bodies (**Figure 9**). These forms also presented a well-developed tubulovesicular membrane network (TMN) in the vacuolar matrix, best seen in **Figure 9A, C**, and **E**. From these multinucleated masses in a certain stage of development of the endopolygeny or schizogony, the merozoites constructed within these masses began to migrate to the periphery, like "budding" on the surface of these structures, being easily recognized by the presence of the emerging conoid, and these stages were identified as type C schizonts (**Figure 9**). **Figure 10** is suggestive of the formation of D-type schizonts, as ascertained by Giemsa-stained light microscopy (**Figure 8A–C**).

Figure 9.
Enterocytes infected with T. gondii bradyzoites of the strain ME-49 for 96 h. Ultrastructure of enterocytes containing type C schizonts. Large vacuoles containing multinucleate mass with the presence of dense granules (DG) and lipids (Li). Tubulovesicular membrane network (TMN) is present in the vacuolar space. Merozoites are seen emerging from the multinucleated masses (arrows). N = nucleus; R = rhoptries. Bars: (A, D, and E) 3 μm; (B and C) 1 μm; (F) 2 μm.

Figure 10.
Enterocytes infected with T. gondii bradyzoites from strain ME-49 for 144 h. Ultrastructure of D-type schizont-containing enterocytes. N = nucleus. Bars: (A) 2 μm; (B) 5 μm.

4. Discussion

The universal distribution of toxoplasmosis and the important role of felines in the transmission of *T. gondii* stimulate research to understand its enteroepithelial cycle better. In this context, the present study employed primary cultures of feline intestinal epithelial cells as a model to investigate the *T. gondii*-host cell interaction.

Some methodological aspects employed in the present study deserve special attention. The use of bradyzoites as a source of infection is justified because it represents one of the natural routes of transmission of *T. gondii* (through the consumption of raw meat by carnivorous animals or humans), based on the hypothesis that the parasite's enteric cycle is most efficient when cats consume tissue cysts (carnivores) [32]. Ferguson, through schematic diagrams, showed all possible routes of development and parasite conversion stages that could occur among the various forms of infection during the life cycle of *T. gondii* [24]. He demonstrated that the only infectious stage capable of direct conversion into merozoites was bradyzoites. These data support the choice of bradyzoites as a source of infection in the present study, making possible the successful differentiation of bradyzoites into merozoites *in vitro*, evidenced by light microscopy and transmission electron microscopy.

In vitro experiments have shown that some parasites initially replicate quickly as tachyzoites to amplify the infection, independent of the infective form (tachyzoites, bradyzoites, or sporozoites) [33]. The conversion of bradyzoites into tachyzoites is a natural process that occurs beginning at 15 h in cell cultures without the addition of immunomodulatory substances [34]. We confirmed this process in FIECs infected with ME49 strain bradyzoites at the 1:5 (parasite: host cell) ratio and, to a smaller extent, 1:10 and 1:20 ratios. It was possible to analyze the intracellular fate of *T. gondii* in the three routes: lytic cycle, cystogenesis, and schizogony in these ratios for periods ranging from 3 to 9 days of interaction.

Our results revealed that decreasing the parasite ratio to 1:10 (bradyzoite: host cell) caused the spontaneous formation of well-defined intracellular cysts in enterocytes after 72 h without any modulation (physical, chemical, or immunological) of the cell culture. Like other researchers, we consider that cystogenesis is a spontaneous event dependent on the strain of *T. gondii*. For example, low-virulent strains (type II) such as ME49 have a natural ability to form cysts in mammalian cells [35–40]. Therefore, we believe that the cell type might be one of the factors that determine the intracellular parasite fate and that intrinsic cellular factors could promote the differentiation stage of *T. gondii* without the need for extrinsic stress factors [41–43].

Here, the occurrence of cystogenesis in feline enterocytes was well characterized ultrastructurally. Our group has already demonstrated in epithelial cells that infection of the feline renal epithelial line CRFK with bradyzoites of strain ME49 (the same strain used in the present study) was more efficient in the establishment of cystogenesis compared to the mouse intestinal epithelial cell line IEC-6 [44]. Our data, combined with the fact that FIEC differentiates in culture, reinforces the concept that cystogenesis *in vitro* is contingent upon several factors, including the strain, parasite load, and cell type (or the interaction of these factors), in addition to the stage of differentiation of the host cells [44–47].

The experimental conditions applied in our experiments using bradyzoites of a low-virulent strain of *T. gondii*, such as ME49, and feline enterocytes allowed us to obtain infective stages corresponding to the morphological characteristics of schizont forms of the parasite, very similar to those characterized *in vivo* [24, 25]. The reproducibility of the sexual cell cycle of *Isospora suis* in intestinal swine epithelial cells was obtained before [48], and it was pointed out the significant influence of the infective dose on the development of intracellular merozoites. The researchers obtained a high density of merozoites when the 1:10 ratio (parasite: host cell) was used and it even allowed the production of oocysts *in vitro* with low parasite loads (1:100 or 1:200). These data are corroborated in part by the results of our group [8] that FIEC

infection with bradyzoites of the ME49 strain using different parasite:host cell ratios was decisive for the intracellular fate of the parasites in enterocytes, in particular, to obtain schizonts. Several experiments were carried out to induce higher production of schizonts in feline enterocytes to, perhaps, obtain sexual forms of *T. gondii*. In this study, we used parasitic load variation, but we were faced with the difficulty of observing a sufficient number of infected cells to allow ultrastructural analysis. We, therefore, chose to infect with the 1:20 load to explore this interaction better. Another strategy also employed was the reduction in the concentration of fetal bovine serum to 1% in the culture medium, as suggested before for *Isospora* [48], but in our system, there was no apparent influence on further induction of schizogony.

Our analysis by optical microscopy of Giemsa-stained monolayers was elucidating because the images of the intracellular stages had a close morphological correlation with the description of schizont stages traditionally reported in the gut of experimentally infected cats [17, 24–26, 49]. The development of schizonts and gametogony in feline enterocytes has been established from the infection of cats with bradyzoites, giving rise to the various stages of *T. gondii* schizonts [49]. It has been postulated that bradyzoites, when penetrating enterocytes, trigger the production of five distinct enteroepithelial stages or schizonts, which are conventionally called types A, B, C, D, and E [25].

The presence of large numbers of multinucleated masses in our enterocyte cultures was the first indication that the *T. gondii* enteroepithelial cycle was established *in vitro*. These structures would correspond to C-type schizonts in the multiple multiplication process, characterized as endopolygeny and/or schizogony by optical microscopic analysis and confirmed by observing the ultrastructure, as proposed by Speer and colleagues [25, 28, 50]. These C-type schizonts are characterized by TMN, mitochondria, electron-dense rhoptries, a large volume of lipids, amylopectin granules, and nuclei displaced to the periphery, as shown in **Figure 9**, in agreement with Speer and Dubey's descriptions [25]. The comparative analysis of the intracellular structures evidenced in enterocytes *in vitro* (**Figure 6A** and **9A**) revealed high similarity with those described by Ferguson [26], who characterized the enteroepithelial stages of histological sections of the intestines of cats. Later stages of the developing schizont type C in enterocyte cultures (**Figure 7**) are similar to those seen in sections of intestinal tissue from infected cats [25], confirming that we were able to partly reproduce the enteroepithelial cycle of *T. gondii in vitro*. Representative images of the schizogony in the process of "budding" of merozoites were observed by electron microscopy (**Figure 9E, F**). When compared to the corresponding ones from this type of schizont described in the original article by Ferguson [26], these images indicate the morphological similarities between these structures. Light and electron microscopic analysis enabled the identification of D-type schizonts, which are also characterized by multinucleated masses that give rise to merozoites from asymmetric nuclear division, which generates organisms with various morphological aspects [17]. Comparing the enterocyte culture images of **Figure 8A** and **10A** with those of histological sections of infected cat intestine [25] shows similarities, indicating that D-type schizonts were produced *in vitro*.

Thus, under our experimental conditions, cultures of FIECs infected with bradyzoites revealed structures very similar to the schizonts of types C and D according to the classification established by Dubey and Frenkel [17] and Speer and Dubey [25] in histological sections of the small intestine of cats orally infected with *T. gondii* cysts.

5. Conclusion

The experimental strategies implemented in this work reproduced *in vitro* the natural cellular microenvironment necessary to establish the enteric development of *T. gondii* in the definitive host, the domestic cat. The primary feline intestinal epithelial cell culture indicated the potential contribution to new approaches for the investigation of parasite cell biology. We demonstrated that analysis of FIECs is an alternative method that could be used to understand the enteric cycle of *T. gondii* under controlled conditions, thereby opening the field for an investigation into the molecular aspects of this interaction. This approach could contribute to the development of new strategies aimed at intervention targeting one of the main routes by which toxoplasmosis spreads.

Acknowledgements

Author details

Renata M. de Muno[1†], Marcos A. Moura[1,2†], Letícia C. Medeiros[1], Pedro N. Caldas[3], Rafael M. Mariante[1] and Helene S. Barbosa[1*]

1 Laboratory of Structural Biology, Oswaldo Cruz Institute, Rio de Janeiro, Brazil

2 School of Medical Sciences and Health of Juiz de Fora, Juiz de Fora, MG, Brazil

3 Veterinary Hospital Niteroi, Niterói, RJ, Brazil

*Address all correspondence to: helene@ioc.fiocruz.br

† These authors contributed equally to this work.

IntechOpen

References

[1] Mahida YR, Galvin AM, Gray T, Makh S, McAlindon ME, Sewell HF, et al. Migration of human intestinal lamina propria lymphocytes, macrophages and eosinophils following the loss of surface epithelial cells. Clinical and Experimental Immunology. 1997;**109**:377-386. DOI: 10.1046/j.1365-2249.1997.4481346.x

[2] Rusu D, Loret S, Peulen O, Mainil J, Dandrifosse G. Immunochemical, biomolecular and biochemical characterization of bovine epithelial intestinal primocultures. BMC Cell Biology. 2005;**6**:42. DOI: 10.1186/1471-2121-6-42

[3] Macartney KK, Baumgart DC, Carding SR, Brubaker JO, Offit PA. Primary murine small intestinal epithelial cells, maintained in long-term culture, are susceptible to rotavirus infection. Journal of Virology. 2000;**74**:5597-5603. DOI: 10.1128/jvi.74.12.5597-5603.2000

[4] Aldhous MC, Shmakov AN, Bode J, Ghosh S. Characterization of conditions for the primary culture of human small intestinal epithelial cells. Clinical and Experimental Immunology. 2001;**125**:32-40. DOI: 10.1046/j.1365-2249.2001.01522.x

[5] Quaroni A. Fetal characteristics of small intestinal crypt cells. Proceedings of the National Academy of Sciences of the United States of America. 1986;**83**:1723-1727. DOI: 10.1073/pnas.83.6.1723

[6] Perreault N, Beaulieu JF. Use of the dissociating enzyme thermolysin to generate viable human normal intestinal epithelial cell cultures. Experimental Cell Research. 1996;**224**:354-364. DOI: 10.1006/excr.1996.0145

[7] Sanderson IR, Ezzell RM, Kedinger M, Erlanger M, Xu ZX, Pringault E, et al. Human fetal enterocytes *in vitro*: Modulation of the phenotype by extracellular matrix. Proceedings of the National Academy of Sciences of the United States of America. 1996;**93**:7717-7722. DOI: 10.1073/pnas.93.15.7717

[8] Moura Mde A, Amendoeira MR, Barbosa HS. Primary culture of intestinal epithelial cells as a potential model for *Toxoplasma gondii* enteric cycle studies. Memórias do Instituto Oswaldo Cruz. 2009;**104**:862-864. DOI: 10.1590/s0074-02762009000600007

[9] Simon-Assmann P, Turck N, Sidhoum-Jenny M, Gradwohl G, Kedinger M. *In vitro* models of intestinal epithelial cell differentiation. Cell Biology and Toxicology. 2007;**23**:241-256. DOI: 10.1007/s10565-006-0175-0

[10] Desmarets LM, Theuns S, Olyslaegers DA, Dedeurwaerder A, Vermeulen BL, Roukaerts ID, et al. Establishment of feline intestinal epithelial cell cultures for the propagation and study of feline enteric coronaviruses. Veterinary Research. 2013;**44**:71. DOI: 10.1186/1297-9716-44-71

[11] Evans GS, Flint N, Potten CS. Primary cultures for studies of cell regulation and physiology in intestinal epithelium. Annual Review of Physiology. 1994;**56**:399-417. DOI: 10.1146/annurev.ph.56.030194.002151

[12] Tenter AM. *Toxoplasma gondii* in animals used for human consumption. Memórias do Instituto Oswaldo Cruz. 2009;**104**:364-369. DOI: 10.1590/s0074-02762009000200033

[13] Schlüter D, Däubener W, Schares G, Groß U, Pleyer U, Lüder C. Animals

are key to human toxoplasmosis. International Journal of Medical Microbiology. 2014;**304**:917-929. DOI: 10.1016/j.ijmm.2014.09.002

[14] Kravetz J. Congenital toxoplasmosis. BMJ. Clinical Evidence. 2013;**2013**:0906

[15] Halonen SK, Weiss LM. Toxoplasmosis. Handbook of Clinical Neurology. 2013;**114**:125-145. DOI: 10.1016/B978-0-444-53490-3.00008-X

[16] Dubey JP, Navarro IT, Sreekumar C, Dahl E, Freire RL, Kawabata HH, et al. *Toxoplasma gondii* infections in cats from Paraná, Brazil: Seroprevalence, tissue distribution, and biologic and genetic characterization of isolates. The Journal of Parasitology. 2004;**90**:721-726. DOI: 10.1645/GE-382R

[17] Dubey JP, Frenkel JK. Cyst-induced toxoplasmosis in cats. The Journal of Protozoology. 1972;**19**:155-177. DOI: 10.1111/j.1550-7408.1972.tb03431.x

[18] Dubey JP. Feline toxoplasmosis and coccidiosis: A survey of domiciled and stray cats. Journal of the American Veterinary Medical Association. 1973;**162**:873-877

[19] Dubey JP, Frenkel JK. Experimental toxoplasma infection in mice with strains producing oocysts. The Journal of Parasitology. 1973;**59**:505-512

[20] Frenkel JK, Dubey JP, Miller NL. *Toxoplasma gondii* in cats: Fecal stages identified as coccidian oocysts. Science. 1970;**167**:893-896. DOI: 10.1126/science.167.3919.893

[21] Ferguson DJ, Hutchison WM, Dunachie JF, Siim JC. Ultrastructural study of early stages of asexual multiplication and microgametogony of *Toxoplasma gondii* in the small intestine of the cat. Acta Pathologica et Microbiologica Scandinavica. Section B: Microbiology and Immunology. 1974;**82**:167-181. DOI: 10.1111/j.1699-0463.1974.tb02309.x

[22] Ferguson DJ, Hutchison WM, Siim JC. The ultrastructural development of the macrogamete and formation of the oocyst wall of *Toxoplasma gondii*. Acta Pathologica et Microbiologica Scandinavica. Section B. 1975;**83**:491-505. DOI: 10.1111/j.1699-0463.1975.tb00130.x

[23] Koyama T, Shimada S, Ohsawa T, Omata Y, Xuan X, Inoue N, et al. Antigens expressed in feline enteroepithelial-stages parasites of *Toxoplasma gondii*. The Journal of Veterinary Medical Science. 2000;**62**:1089-1092. DOI: 10.1292/jvms.62.1089

[24] Ferguson DJ. Use of molecular and ultrastructural markers to evaluate stage conversion of *Toxoplasma gondii* in both the intermediate and definitive host. International Journal for Parasitology. 2004;**34**:347-360. DOI: 10.1016/j.ijpara.2003.11.024

[25] Speer CA, Dubey JP. Ultrastructural differentiation of *Toxoplasma gondii* schizonts (types B to E) and gamonts in the intestines of cats fed bradyzoites. International Journal for Parasitology. 2005;**35**:193-206. DOI: 10.1016/j.ijpara.2004.11.005

[26] Ferguson DJ. *Toxoplasma gondii*: 1908-2008, homage to Nicolle, Manceaux and Splendore. Memórias do Instituto Oswaldo Cruz. 2009;**104**:133-148. DOI: 10.1590/s0074-02762009000200003

[27] Mehran M, Levy E, Bendayan M, Seidman E. Lipid, apolipoprotein, and lipoprotein synthesis and secretion during cellular differentiation in Caco-2 cells. In Vitro Cellular & Developmental

Biology. Animal. 1997;**33**:118-128. DOI: 10.1007/s11626-997-0032-3

[28] Freyre A. Separation of toxoplasma cysts from brain tissue and liberation of viable bradyzoites. The Journal of Parasitology. 1995;**81**:1008-1010

[29] Guimarães EV, Acquarone M, de Carvalho L, Barbosa HS. Anionic sites on *Toxoplasma gondii* tissue cyst wall: Expression, uptake and characterization. Micron. 2007;**38**:651-658. DOI: 10.1016/j.micron.2006.09.002

[30] Popiel I, Gold MC, Booth KS. Quantification of *Toxoplasma gondii* bradyzoites. The Journal of Parasitology. 1996;**82**:330-332

[31] Bohne W, Gross U, Ferguson DJ, Heesemann J. Cloning and characterization of a bradyzoite-specifically expressed gene (hsp30/bag1) of *Toxoplasma gondii*, related to genes encoding small heat-shock proteins of plants. Molecular Microbiology. 1995;**16**:1221-1230. DOI: 10.1111/j.1365-2958.1995.tb02344.x

[32] Dubey JP. Comparative infectivity of oocysts and bradyzoites of *Toxoplasma gondii* for intermediate (mice) and definitive (cats) hosts. Veterinary Parasitology. 2006;**140**:69-75. DOI: 10.1016/j.vetpar.2006.03.018

[33] Dubey JP. Survival of *Toxoplasma gondii* tissue cysts in 0.85-6% NaCl solutions at 4-20°C. The Journal of Parasitology. 1997;**83**:946-949

[34] Gross U, Bohne W, Lüder CG, Lugert R, Seeber F, Dittrich C, et al. Regulation of developmental differentiation in the protozoan parasite *Toxoplasma gondii*. The Journal of Eukaryotic Microbiology. 1996;**43**:114S-116S. DOI: 10.1111/j.1550-7408.1996.tb05033.x

[35] McHugh TD, Gbewonyo A, Johnson JD, Holliman RE, Butcher PD. Development of an *in vitro* model of *Toxoplasma gondii* cyst formation. FEMS Microbiology Letters. 1993;**114**:325-332. DOI: 10.1111/j.1574-6968.1993.tb06593.x

[36] Dardé ML, Bouteille B, Leboutet MJ, Loubet A, Pestre-Alexandre M. *Toxoplasma gondii*: étude ultrastructurale des formations kystiques observées en culture de fibroblastes humains [*Toxoplasma gondii*: Ultrastructural study of cystic formations observed in human fibroblast culture]. Annales de Parasitologie Humaine et Comparée. 1989;**64**:403-411. French. DOI: 10.1051/parasite/1989646403

[37] Lindsay DS, Dubey JP, Blagburn BL, Toivio-Kinnucan M. Examination of tissue cyst formation by *Toxoplasma gondii* in cell cultures using bradyzoites, tachyzoites, and sporozoites. The Journal of Parasitology. 1991;**77**:126-132

[38] Guimarães EV, de Carvalho L, Barbosa HS. Primary culture of skeletal muscle cells as a model for studies of *Toxoplasma gondii* cystogenesis. The Journal of Parasitology. 2008;**94**:72-83. DOI: 10.1645/GE-1273.1

[39] Guimarães EV, Carvalho L, Barbosa HS. Interaction and cystogenesis of *Toxoplasma gondii* within skeletal muscle cells *in vitro*. Memórias do Instituto Oswaldo Cruz. 2009;**104**:170-174. DOI: 10.1590/s0074-02762009000200007

[40] de Muno RM, Moura MA, de Carvalho LC, Seabra SH, Barbosa HS. Spontaneous cystogenesis of *Toxoplasma gondii* in feline epithelial cells *in vitro*. Folia Parasitol (Praha). 2014;**61**:113-119

[41] da Silva F, Mda F, Barbosa HS, Gross U, Lüder CG. Stress-related

and spontaneous stage differentiation of *Toxoplasma gondii*. Molecular BioSystems. 2008;**4**:824-834. DOI: 10.1039/b800520f

[42] Ferreira-da-Silva Mda F, Rodrigues RM, Andrade EF, Carvalho L, Gross U, Lüder CG, et al. Spontaneous stage differentiation of mouse-virulent *Toxoplasma gondii* RH parasites in skeletal muscle cells: An ultrastructural evaluation. Memórias do Instituto Oswaldo Cruz. 2009;**104**:196-200. DOI: 10.1590/s0074-02762009000200012

[43] Ferreira-da-Silva Mda F, Takács AC, Barbosa HS, Gross U, Lüder CG. Primary skeletal muscle cells trigger spontaneous *Toxoplasma gondii* tachyzoite-to-bradyzoite conversion at higher rates than fibroblasts. International Journal of Medical Microbiology. 2009;**299**:381-388. DOI: 10.1016/j.ijmm.2008.10.002

[44] Molestina RE, El-Guendy N, Sinai AP. Infection with *Toxoplasma gondii* results in dysregulation of the host cell cycle. Cellular Microbiology. 2008;**10**:1153-1165. DOI: 10.1111/j.1462-5822.2008.01117.x

[45] Lavine MD, Arrizabalaga G. Induction of mitotic S-phase of host and neighboring cells by *Toxoplasma gondii* enhances parasite invasion. Molecular and Biochemical Parasitology. 2009;**164**:95-99. DOI: 10.1016/j.molbiopara.2008.11.014

[46] Kim MJ, Jung BK, Cho J, Song H, Pyo KH, Lee JM, et al. Exosomes secreted by *Toxoplasma gondii*-infected L6 cells: Their effects on host cell proliferation and cell cycle changes. The Korean Journal of Parasitology. 2016;**54**:147-154. DOI: 10.3347/kjp.2016.54.2.147

[47] Worliczek HL, Ruttkowski B, Schwarz L, Witter K, Tschulenk W, Joachim A. *Isospora suis* in an epithelial cell culture system - an *in vitro* model for sexual development in coccidia. PLoS One. 2013;**8**:e69797. DOI: 10.1371/journal.pone.0069797

[48] Dubey JP, Miller NL, Frenkel JK. *Toxoplasma gondii* life cycle in cats. Journal of the American Veterinary Medical Association. 1970;**157**:1767-1770

[49] Speer CA, Dubey JP, Blixt JA, Prokop K. Time lapse video microscopy and ultrastructure of penetrating sporozoites, types 1 and 2 parasitophorous vacuoles, and the transformation of sporozoites to tachyzoites of the VEG strain of *Toxoplasma gondii*. The Journal of Parasitology. 1997;**83**:565-574

[50] Speer CA, Clark S, Dubey JP. Ultrastructure of the oocysts, sporocysts, and sporozoites of *Toxoplasma gondii*. The Journal of Parasitology. 1998;**84**:505-512